

Extreme Value Statistics of the Total Energy in an  
Intermediate Complexity Model of the  
Mid-latitude Atmospheric Jet.  
Part II: trend detection and assessment.

Mara Felici<sup>1,2</sup>, Valerio Lucarini<sup>1</sup>, Antonio Speranza<sup>1</sup>, Renato Vitolo<sup>1, \*</sup>

November 26, 2006

<sup>1</sup> *PASEF – Physics and Applied Statistics of Earth Fluids,  
Dipartimento di Matematica ed Informatica, Università di Camerino*

<sup>2</sup> *Dipartimento di Matematica U. Dini, Università di Firenze*

---

*\*Corresponding author address:* Dr. Renato Vitolo, Department of Mathematics and Informatics, University of Camerino, via Madonna delle Carceri, 62032 Camerino (MC), Italy.  
E-mail: renato.vitolo@unicam.it

## Abstract

A baroclinic model for the atmospheric jet at middle-latitudes is used as a stochastic generator of non-stationary time series of the total energy of the system. A linear time trend is imposed on the parameter  $T_E$ , descriptive of the forced equator-to-pole temperature gradient and responsible for setting the average baroclinicity in the model. The focus lies on establishing a theoretically sound framework for the detection and assessment of trend at extreme values of the generated time series. This problem is dealt with by fitting time-dependent Generalized Extreme Value (GEV) models to sequences of yearly maxima of the total energy. A family of GEV models is used in which the location  $\mu$  and scale parameters  $\sigma$  depend quadratically and linearly on time, respectively, while the shape parameter  $\xi$  is kept constant. From this family, a model is selected by using diagnostic graphical tools, such as probability and quantile plots, and by means of the likelihood ratio test. The inferred location and scale parameters are found to depend in a rather smooth way on time and, therefore, on  $T_E$ . In particular, power-law dependences of  $\mu$  and  $\sigma$  on  $T_E$  are obtained, in analogy with the results of a previous work where the same baroclinic model was run with fixed values of  $T_E$  spanning the same range as in this case. It is emphasized under which conditions the adopted approach is valid.

PACS: 02.50.Tt, 02.70.-c, 47.11.-j, 92.60.Bh, 92.70.Gt

# 1. Introduction

In the context of Climate Change, an intensely debated question is whether the statistics of extreme meteo-climatic events is changing (and/or will change) and, in case, how fast it is changing (and/or will change). For example, the role of time-dependence in the statistics of extreme weather events has been at the heart of discussions about climate change since the work by Katz and Brown (1992). In particular, the detection of trends in the frequency of intense precipitation has been the object of much research, particularly at regional level, see *e.g.* Karl et al. (1996); Karl and Knight (1998) for the USA and Brunetti et al. (2002, 2004) for the Mediterranean area. The general relevance of the problem has been highlighted in the 2002 release of a specific IPCC report on *Changes in extreme weather and climate events* (available at <http://www.ipcc.ch/pub/support.htm>). In fact, the emphasis laid on the subject by the IPCC report reverberated in many countries the question “is the probability of major impact weather increasing?”. This question reached the big public almost everywhere and innumerable studies of trends in series of “extremes” were undertaken. These studies mainly deal with variables of *local character*, typically precipitation and temperature at specific stations. Moreover, most studies are regional: see *e.g.* the proceedings of the Italia-USA meeting held in Bologna in 2004 (Diaz and Nanni 2006) for the relevance of the extreme events in the Mediterranean Climates and the INTERREG IIIB - CADSES project HYDROCARE, <http://www.hydrocare-cadses.net>, for impacts of extreme events in the hydrological cycle of the central-eastern Europe.

In a preceding, companion paper (Felici et al. 2006) (which we refer to by Part I in the sequel) we have addressed the problem of extreme value statistical inference on statistically *stationary* time series produced by a dynamical system providing a minimal model for the dynamics of the mid-latitudes baroclinic jet. There reported is, from mathematical literature, a suitable, rigorous, “universal” setting for the analysis of the extreme events in stationary time series. This is based on Gnedenko’s theorem (Gnedenko 1943) according to which the distribution of the block-maxima of a sample of independent identically distributed variables converges, under fairly mild assumptions, to a member of a three-real parameter family of distributions, the so-called Generalized Extreme Value (GEV) distribution (Coles 2001). The GEV approach to the analysis of extremes requires that three basic conditions are met, namely the *independence* of the selected extreme values, the consideration of a *sufficiently large* number of extremes, the selection of values that are *genuinely* extreme. This could be performed relatively easily for the case at hand.

Part I was originally motivated by the interest in weather having “major impact” (on human life and property) in the Mediterranean area, in particular intense precipitation and heat waves over Italy. See, for example, Brunetti et al. (2002, 2004); Lucarini et al. (2004, 2006b); Speranza et al. (2006); Speranza and Tartaglione (2006); Tartaglione et al. (2006) and the MEDEX Phase 1 report (available at <http://medex.inm.uib.es/>) for related results and activities. The study reported in Part I has revealed, among other things, that diagnostics of extreme statistics can highlight interesting dynamical properties of the analyzed system. Properties which, thanks to the “universality of the GEV”, can be

investigated in a low dimensionality space of parametric probability density functions, although at the expenses of the total length of the observational record of the system in order to capture a sufficient number of independent extremes. A key role (that is presently being explored elsewhere, in the context of general atmospheric circulation theory) was played in Part I by the smoothness of variation of the extreme statistics parameters (average, variance, shape factor) upon the external (forcing) parameters of the system. In this paper, again, we devote attention to exploring the statistics of extremes as a dynamical indicator, this time in the framework of the (typically meteorological) statistical inference problem of detecting trends in observations.

The definition of a rigorous approach to the study of extremes is much harder when the property of stationarity does not hold. One basic reason is that there exists no universal theory of extreme values (such as *e.g.* a generalization of Gnedenko's theorem) for non-stationary stochastic processes. Moreover, in the analysis of observed or synthetically generated sequences of data of finite length, practical issues, such as the possibility of unambiguously choosing the time scales which defines the statistical properties and their changes, become of critical importance. Nevertheless, GEV-based statistical modeling offers a practical unified framework also for the study of extremes in non-stationary time series. In the applications, the three parameters of the GEV distribution are taken as time-dependent and time is introduced as a covariate in the statistical inference procedure (Coles 2001). The practical meaning of this assumption is that the probability of occurrence (chance) of the considered extreme events evolves in time pretty much as we

are inclined to think in our everyday life. However, giving a scientific meaning to such an assumption is possible only in an intuitive, heuristical fashion: in an “adiabatic” limit of infinitely slow trends (but rigorously not even in such a limit). We adopt this point of view not only because it is in line with the common practice and view of extremes, but also because interesting dynamical properties can be inferred from extremes, in analogy with the findings in Part I.

In the present paper we perform and assess time-dependent GEV inference on non-stationary time series  $E(t)$  of the total energy obtained by the same simplified quasi-geostrophic model that was used in Part I. The model undergoes baroclinic forcing towards a given latitudinal temperature profile controlled by the forced equator-to-pole temperature difference  $T_E$ ; see Lucarini et al. (2006c,d) for a thorough description. We analyze how the parameters of the GEV change with time when a linear trend is imposed on the large scale macroscopic forcing  $T_E$ , that is, when  $T_E$  is taken as a (linear) function of time. Since this functional relation is invertible, we derive a parametrization relating the changes in the GEV to variations in  $T_E$  (instead of time). One major goal here is to present a methodological framework to be adopted with more complex models and with data coming from observations, as well as an assessment of the performance of the GEV approach for the analysis of trends in extremes in the somewhat *grey area* of non-stationary time series. Methodologically, our set-up is somewhat similar to that of Zhang et al. (2003) regarding the procedures of statistical inference. However, in this case we face two additional problems:

1. as in Part I, the statistical properties of the time series  $E(t)$  cannot be selected *a priori*: in the stationary case ( $T_E$  constant in time) and much less in the non-stationary case there is no explicit formula for the probability distribution of the observable  $E(t)$ ;
2. moreover, in the non-stationary case we even lack a *definition* (and in fact a mere *candidate*) of what might be the probability distribution of  $E(t)$ : certainly not a frequency limit for  $t \rightarrow \infty$  (and not by construction, as opposed to Zhang et al. (2003) who use genuinely stochastic generators).

This also means that we have no hypothesis concerning the functional form of the trend in the statistics of extremes of  $E(t)$ , resulting from the trend imposed on the control parameter  $T_E$ . The lack of a general GEV theorem for non-stationary sequences implies that the choice of the time-dependent GEV as a statistical model is, in principle, arbitrary: other models might be equally (or better) suitable. Here comes into play the “adiabaticity” hypothesis mentioned above, which leads to the central statement of this paper: if the trend is sufficiently slow and if the statistical behaviour of the atmospheric model has a sufficiently regular response with respect to variations in the external parameters, the GEV remains a suitable model for inference of trend in extremes.

The structure of the paper follows. In Sec. 2 we describe the general problem of the characterization of statistical trends in deterministic models, with both its conceptual and practical implications. Then in Sec. 3 we describe how the GEV modeling can be applied

to non-stationary time-series and how the quality-check of the fits is performed. In section Sec. 4 we present the time series considered in this work and the set-up of the numerical experiments performed with the atmospheric model. The inferences for various values of the trend in the forcing parameter  $T_E$  are presented in Sec. 5 and a sensitivity analysis is carried out in Sec. 6. Comparison with the stationary case analyzed in Part I is given in Sec. 7. In Sec. 8, finally, we summarize the main findings of this work, highlighting the future research developments.

## 2. Statistical trends: the theoretical problem

The stochastic generator used in this paper to produce the time series is a deterministic model (an ordinary differential equation), whose dynamics, for the considered range of values of  $T_E$ , is chaotic in the sense that it takes place on a strange attractor  $\Lambda$  in phase space (Eckmann and Ruelle 1985). See Lucarini et al. (2006c,d) for a study of the properties of this attractor, including sensitivity with respect to initial conditions. The statistical behaviour of this type of time series is determined by the Sinai-Ruelle-Bowen (SRB) probability measure  $\mu$  (Eckmann and Ruelle 1985): this is a Borel probability measure in phase space which is invariant under the flow  $f^t$  of the differential equation, is ergodic, is singular with respect to the Lebesgue measure in phase space and its conditional measures along unstable manifolds are absolutely continuous, see Young (2002) and references therein. Moreover, the SRB measure is also a *physical measure*: there is a set  $V$



having full Lebesgue measure in a neighbourhood  $U$  of  $\Lambda$  such that for every continuous observable  $\phi : U \rightarrow \mathbb{R}$ , we have, for every  $x \in V$ , the frequency-limit characterization

$$\lim_{t \rightarrow \infty} \frac{1}{t} \int_0^t \phi(f^t(x)) dt = \int \phi d\mu. \quad (1)$$

Existence and uniqueness of an SRB measure  $\mu$  have been proved only for very special classes of flows  $f^t$  (in particular, for flows that possess an Axiom-A attractor, see Young (2002)). However, existence and uniqueness of  $\mu$  are *necessary* to define a stationary stochastic process associated to an observable  $\phi$ . In turn, this allows to consider a given time series of the form  $\phi(f^t(x)) : t > 0$  as a realization of the stationary process, justifying statistical inference on a solid theoretical basis. In part I, we conjectured existence and uniqueness of an SRB measure for the atmospheric model, providing the theoretical foundation to the application of GEV models in the inference of extreme values.

In certain cases of non-autonomous ordinary differential equations (for example, if the dependence on time is periodic), it still is possible to define, at least conceptually, what an SRB measure is. However, in the present case, due to the form of time-dependence adopted for the parameter  $T_E$ , the atmospheric model admits *no invariant measure*. This means that there is no (known) way to associate a stochastic process to the time series of the total energy. In other words, it is even in doubt what we mean by “statistical properties” of the time series, since it is *impossible* to define a probability distribution. This conceptual problem has a very serious practical consequence: the “operational”

definition of probability as a frequency limit (as in (1)) *is not valid in the non-stationary case*, since the time evolution is not a sampling of a unique probability distribution. Even if one assumes the existence of a sequence of distinct probability distributions, one for each observation, one realization (the time series) does not contain sufficient statistical information, since each distribution is very undersampled (with only one observation).

Despite all these problems, the results in Part I suggest a framework which is, for the moment, formulated in a heuristic way. Suppose you evolve an initial condition  $x$  in phase space by the flow  $f^t$  of the *autonomous* atmospheric model, that is the system in which  $T_E$  is kept fixed to some value  $T_E^0$ . After an initial time span (transient), say for  $t$  larger than some  $t_0 > 0$ , the evolution  $f^t(x)$  may be thought to take place on the attractor  $\Lambda$  and time-averages of the form

$$\frac{1}{t - t_0} \int_{t_0}^t \phi(f^t(x)) dt \quad (2)$$

may be considered as approximations of

$$\int \phi d\mu_0, \quad (3)$$

which is the average of  $\phi$  by the SRB measure  $\mu_0$  existing at the value  $T_E = T_E^0$  (the “attractor average” at  $T_E^0$ ). Now suppose that at some  $t_1 > t_0$  the parameter  $T_E$  is abruptly changed to some value  $T_E^1 > T_E^0$ : there will be some transient interval, call it  $[t_1, t_2]$ ,

during which the evolution  $f^t(x)$  approaches the *new* attractor of the atmospheric model, that is the attractor existing for  $T_E$  fixed at  $T_E^1$ . After that time span, the evolution may be considered to take place on the new attractor.

In our case, though  $T_E$  varies continuously (linearly) with time, if the trend magnitude is low, then  $T_E$  may be considered constant (with good approximation) during time spans that are sufficiently long in order to have both convergence to the “new” attractor and good sampling of the “new” SRB measure, in the sense sketched above. Though admittedly heuristic, this scenario allows to clarify under which condition it is still reasonable to speak of “statistical properties” of a time series generated by a non-autonomous system: namely, the closeness to a stationary situation for time spans that are sufficiently long. This is the “adiabatic” hypothesis which we mentioned in the introduction. An essential ingredient for this to hold is that the statistical properties of the autonomous model *do not sensibly depend on the external parameter*  $T_E$ , in the sense that no abrupt transitions (bifurcations) should take place as  $T_E$  is varied. This was indeed checked for the system at hand in Part I. Notice that the validity of the “adiabatic” hypothesis also has a useful practical consequence: one can use the statistics of the stationary system as a reference against which the results for the non-stationary case can be assessed. Having this scenario in mind, we proceed to the description of the time-dependent GEV approach in the next section.

### 3. GEV modelling for non-stationary time series

#### 3a. Stationary case

The GEV approach for sequences of independent, identically distributed (i.i.d.) random variables is by now rather standard (Castillo 1988; Coles 2001; Embrechts et al. 1997; Falk et al. 1994; Galambos 1978; Gumbel 1958; Jenkinson 1955; Lindgren et al. 1983; Reiss and Thomas 2001; Tiago de Oliveira 1984). The foundation is Gnedenko's theorem (Gnedenko 1943; Fisher and Tippett 1928). Consider a time series, assumed to be a realization of a sequence of i.i.d. random variables. The time series is divided into  $m$  consecutive time-frames (data blocks), each containing  $n$  subsequent observations, equally spaced in time. Denote by  $z_1, \dots, z_m$  the sequence of the block maxima taken over each time-frame. Under fairly mild assumptions, the distribution of the block-maxima converges, in a suitable limit involving a rescaling, to the GEV distribution, defined as

$$G(x; \mu, \sigma, \xi) = \exp \left\{ - \left[ 1 + \xi \left( \frac{x - \mu}{\sigma} \right) \right]^{-1/\xi} \right\} \quad (4)$$

for all  $x$  in the set  $\{x : 1 + \xi(x - \mu)/\sigma > 0\}$  and  $G(x) = 0$  otherwise, where  $\sigma > 0$  and  $\xi \neq 0$ . If  $\xi = 0$  the limit distribution is the Gumbel distribution

$$G(x; \mu, \sigma, 0) = \exp \left( - \exp \left( - \frac{x - \mu}{\sigma} \right) \right), \quad x \in \mathbb{R}. \quad (5)$$

GEV inference consists in estimating the distributional parameters  $(\mu, \sigma, \xi)$  (called location, scale and shape parameter, respectively) from the available data. A widely used technique consists in numerically maximizing the *log-likelihood* function  $l(\mu, \sigma, \xi)$ . For  $\xi \neq 0$ , this is defined as

$$l(\mu, \sigma, \xi) = -m \log \sigma - \left(1 + \frac{1}{\xi}\right) \sum_{t=1}^m \left\{ \log \left[ 1 + \xi \left( \frac{z_t - \mu}{\sigma} \right) \right] - \left[ 1 + \xi \left( \frac{z_t - \mu}{\sigma} \right) \right]^{-\frac{1}{\xi}} \right\}, \quad (6)$$

while an analogous formula holds for  $\xi = 0$  (Coles 2001).

A generalization of the GEV theorem holds for time series that are realizations of stationary stochastic processes such that the long-range dependence is weak at extreme levels (Leadbetter 1974, 1983). In the applications, this property is assumed to hold whenever the block maxima are uncorrelated for sufficiently large block sizes. In this case, GEV inference and assessment is carried out by the same tools (maximum likelihood, diagnostic plots, etc.) used in the i.i.d. context, see Coles (2001).

### **3b. Time-dependent case**

If stationarity of the time series does not hold, then the limiting distribution function is no longer bound to be the GEV or any other family (4): no theories of extreme values exist in this context. Some exact results are known only in certain very specialized types of

non-stationarity (Hüsler 1986; Lindgren et al. 1983), but it is very unlikely that a general theory can be established. However, GEV-based statistical modeling of extreme values can be performed also in the case of time-dependent phenomena by adopting a pragmatic approach, where the GEV distribution (4) is used as a template: time-dependent parameters  $\mu(t)$  and  $\sigma(t)$  are considered, yielding a GEV model of the form

$$G(x; \mu(t), \sigma(t), \xi). \quad (7)$$

Usually  $\xi$  is kept time-independent in order to avoid numerical problems, since it is usually the most delicate parameter to estimate (Coles 2001). Different kinds of time-dependence can be imposed for  $(\mu(t), \sigma(t))$ . In this paper, we adopt a simple polynomial family of models:

$$\mu(t) = \mu_0 + \mu_1 t + \mu_2 t^2, \quad \sigma(t) = \sigma_0 + \sigma_1 t, \quad (8)$$

with  $\mu_{0,1,2}$  and  $\sigma_{0,1} \in \mathbb{R}$ . GEV models in family (8) are denoted by  $G_{p,q}$ , with  $0 \leq p \leq 2$  and  $0 \leq q \leq 1$ , where  $p$  and  $q$  denote the maximum degree of  $t$  in  $\mu(t)$  and in  $\sigma(t)$ , respectively. The time-dependent GEV model (7) constructed in this way is a generalization of (4) (the latter is obtained by setting  $\mu_1 = \mu_2 = \sigma_1 = 0$  in (8)). For model (7) with parameters (8), GEV inference amounts to estimating the parameter

vector

$$\boldsymbol{\beta} = [\mu_0, \mu_1, \mu_2, \sigma_0, \sigma_1, \xi] \quad (9)$$

by including time  $t$  as a covariate.

Suppose we have a non-stationary dataset, from which a sequence of block maxima  $z_t$ , with  $t = 1, \dots, m$ , is constructed. A log-likelihood function for the case  $\xi \neq 0$  is defined as

$$l(\boldsymbol{\beta}) = - \sum_{t=1}^m \left\{ \log \sigma(t) + (1 + 1/\xi) \log \left[ 1 + \xi \left( \frac{z_t - \mu(t)}{\sigma(t)} \right) \right] + \left[ 1 + \xi \left( \frac{z_t - \mu(t)}{\sigma(t)} \right) \right]^{-1/\xi} \right\} \quad (10)$$

(compare with (6)), provided that

$$1 + \xi \left( \frac{z_t - \mu(t)}{\sigma(t)} \right) > 0, \quad i = 1, \dots, m. \quad (11)$$

If  $\xi = 0$ , an alternative log-likelihood function, derived from the Gumbel distribution, must be used (Coles 2001). Numerical procedures are used to maximize the selected log-likelihood function, yielding the maximum likelihood estimate of the parameter vector  $\boldsymbol{\beta}$ . Confidence intervals for  $\boldsymbol{\beta}$  may be computed by the expected or observed information matrix (Coles 2001).

Of course, all of the above procedure is performed in the spirit of “pure” inference,

that is determining the likelihood of the adopted parametric hypothesis and *not* its truth which, in the absence of a supporting theorem, remains unknown. Moreover, it should be kept in mind that several different models might fit the observations with similar reliability (likelihood). In this case, as no *universal* model is suggested or enforced (as opposed to the stationary case), there is no reason to prefer the one above the other.

### 3c. Assessment of statistical models

In the non-stationary context the analysis starts from a list of models ( $G_{p,q}$  in our case, see (8)) which we fit to the data searching for the most adequate one. Assessment and comparisons of the inferences are based on standard graphical tools such as *probability plot*, *quantile plot*, and the *likelihood ratio test*. However, for the graphical model-checking the non-stationarity must be taken into account. Reduction to *Gumbel scale* is a practical way to treat this problem (Coles 2001).

Let  $z_t, t = 1, \dots, m$  be a sequence of block maxima extracted from a non-stationary time series, from which the time-dependent GEV model  $G(\hat{\mu}(t), \hat{\sigma}(t), \hat{\xi})$  has been fitted as described in the previous section. The sequence of maxima is transformed according to

$$\tilde{z}_t = \log \left[ \left( 1 + \hat{\xi} \left( \frac{z_t - \hat{\mu}(t)}{\hat{\sigma}(t)} \right) \right)^{-\frac{1}{\hat{\xi}}} \right], \quad t = 1, \dots, m. \quad (12)$$

If  $Z_t$  are random variables with distribution  $G(\hat{\mu}(t), \hat{\sigma}(t), \hat{\xi})$ , then the transformation (12)



produces variables  $\tilde{Z}_t$  that have the standard Gumbel distribution:

$$P(\tilde{Z}_t < x) = \exp(-e^{-x}), \quad x \in \mathbb{R}, \quad (13)$$

which is the GEV with parameters  $(\mu, \sigma, \xi) = (0, 1, 0)$ . Therefore, transformation (12) attempts to remove the time-dependence from the sequence of maxima, bringing it as close as possible to the common scale given by the standard Gumbel distribution (13). This way, the distribution function and the quantiles of the transformed sequence of maxima  $\tilde{z}_t$  can be compared with the empirical ones derived from (13). The probability plot is a graph of the pairs

$$\left( \frac{j}{m+1}; \exp(-e^{-\tilde{z}_{(j)}}) \right), \quad j = 1, \dots, m, \quad (14)$$

where  $\tilde{z}_{(1)} \leq \tilde{z}_{(2)} \leq \dots \leq \tilde{z}_{(m)}$  is the order statistics of the transformed sequence of maxima  $\tilde{z}_t$ . The quantile plot is given by the pairs

$$\left( -\log \left( -\log \left( \frac{j}{m+1} \right) \right); \tilde{z}_{(j)} \right), \quad j = 1, \dots, m. \quad (15)$$

For both plots, displacement of points from the diagonal indicates low quality of the inference.

The **likelihood ratio test** is used to compare the goodness-of-fit of two *nested models*, that is, two models such that one of them is a sub-model (a particular case) of the other

one. Our family  $G_{p,q}$  of models is nested: for example  $G_{1,0}$  is a sub-model of  $G_{2,1}$ , obtained by setting  $\mu_2$  and  $\sigma_1$  to zero in the parameter vector  $\beta$  defined in (9). Given integers  $0 \leq p_1 \leq p_2 \leq 2$  and  $0 \leq q_1 \leq q_2 \leq 1$ , let  $l_1$  and  $l_2$  be the maximized values of the log-likelihood (10) for the nested models  $G_{p_1,q_1}$  and  $G_{p_2,q_2}$ , respectively, and define the **deviance statistic** as

$$\mathcal{D} = 2\{l_2 - l_1\}. \quad (16)$$

The likelihood ratio test states that the simpler model  $G_{p_1,q_1}$  is to be rejected at the  $\alpha$ -level of confidence in favor of  $G_{p_2,q_2}$  if  $\mathcal{D} > c_\alpha$ , where  $c_\alpha$  is the  $(1 - \alpha)$ -quantile of the  $\chi_k^2$  distribution and  $k$  is the number of parameters that belong to  $G_{p_2,q_2}$  and that are null in  $G_{p_1,q_1}$  ( $k = 2$  in our example above).

Although the number of time-dependent models one may choose from is virtually infinite, parsimony in the construction is recommended (Coles 2001): too many coefficients in the functions  $(\mu(t), \sigma(t))$  would result in unacceptably large uncertainties, especially if few data are available. The search of the best model is carried out by trial-and-error: the choice of a more complex model should be strongly justified on theoretical grounds or by a significantly higher accuracy (that is,  $\mathcal{D}$  exceedingly larger than  $c_\alpha$  for nested models). However, the convergence of the above described procedure is *by no means* a guarantee of good estimate of the “true” probability density function: the latter is conceptually *undefined*. See our remarks at the end of Sec. 3b.

## 4. The time series: Total Energy of the Atmospheric Jet

### Model with a trend in average baroclinicity

We consider here the same baroclinic jet model used in Part I, where the spectral order  $JT$  is set to 32. The model temperature is relaxed towards a given equator-to-pole profile which acts as baroclinic forcing. The statistical properties of the model radically change when the parameter  $T_E$ , determining the forced equator-to-pole temperature gradient, is varied. A physical and dynamical description of the model is given in Speranza and Malguzzi (1988); Malguzzi et al. (1990); Lucarini et al. (2006c,d).

In Part I we performed an extreme value analysis of the system's response with respect to variations in  $T_E$ . Several stationary time series of the total energy  $E(t)$  were used as a basis for GEV inference. Each time series was generated with  $T_E$  fixed at one value within a uniform grid on the interval  $[10, 50]$ , with spacing of 2 units. We recall that, given the non-dimensionalization of the system,  $T_E = 1$  corresponds to 3.5 K, 1 unit of total energy corresponds to roughly  $5 \times 10^{17}$  J, and  $t = 0.864$  is one day, see Lucarini et al. (2006c,d). In that case, all parameters of the system being kept fixed, after discarding an initial transient each time series of the total energy could be considered as a realization of a stationary stochastic process having weak long-range dependence. Therefore, the classical framework for GEV modeling was applied (see Sec. 3a).

In the present setting, a specific linear trend is imposed on  $T_E$ : starting at time  $t = 0$ ,

the model is run with a the time-dependent forcing parameter

$$T_E(t) = (T_E^0 - 1) + t \Delta T_E, \quad t \in [0, t_0], \quad (17)$$

with  $T_E^0 = 10$ . Three values are chosen for the trend intensity  $\Delta T_E$ : 2 units every  $L_B = 1000, 300, \text{ and } 100$  years, yielding three time series for the total energy  $E(t)$ . The range swept by  $T_E(t)$  during integration is kept fixed in all three cases to the interval  $[9, 51]$ , so that the total length of the time series depends on  $\Delta T_E$ . Each time series is split into 21 data blocks  $B^i, i = 1, \dots, 21$ . The length  $L_B$  of each block corresponds to a time interval  $I^i$  such that, as  $t$  varies within  $I^i$ , the baroclinicity parameter  $T_E(t)$  by (17) spans the interval

$$[T_E^i - 1, T_E^i + 1], \quad (18)$$

which is 2 units wide and centered around one of the values  $T_E^i$  considered in Part I:

$$(T_E^0, T_E^1, \dots, T_E^{21}) = (10, 12, 14, \dots, 50). \quad (19)$$

Therefore, the total length  $L$  of the time series depends on the trend intensity, so that we have  $L = 21 \times 2 / \Delta T_E = 21 L_B$ . Moreover, since the time-span over which the maxima are computed is kept fixed to one year, the number of maxima in each data block  $B^i$  also depends on  $\Delta T_E$ : in fact, it is equal to  $L_B$ , see Tab. 1.

Such a selection of the intervals as in (18) allows for a direct comparison of the present

results with those obtained for stationary time series in Part I. Moreover, our choices regarding block length and other factors are based on the indications provided in Part I, where the goodness-of-fit assessments performed by a variety of means showed that:

- the adopted block length of one year makes sure that the extremes are uncorrelated and *genuinely extreme*;
- the minimum length (100 data) used for the sequences of maxima yields robust inferences.

## 5. Time-dependent GEV Analysis of the Total Energy

For each data block  $B^i$ ,  $i = 1, \dots, 21$ , we first extract a sequence of yearly maxima  $z_t^i$ , with  $t = 1, \dots, L_B$ . For compactness, each sequence is denoted in vector form as  $\mathbf{z}^i = (z_1^i, z_2^i, \dots, z_{L_B}^i)$ . One GEV model of the form  $G_{p,q}$  (see (8)) is fitted from each of the sequences  $\mathbf{z}^i$ . For each  $i = 1, \dots, 21$ , the analysis follows three main steps:

1. nested models  $G_{p,q}$ , for  $0 \leq p \leq 2$  and  $0 \leq q \leq 1$ , are fitted on the  $i$ -th sequence of maxima  $\mathbf{z}^i$ ;
2. models with too low maximum likelihood are discarded and the deviance test is applied to the others to select the best estimate model;
3. the best estimate model is graphically checked by examining the probability and quantile plots, and it is possibly rejected in favor of a model having less nonzero

parameters in the vector  $\beta$  as in (9).

Following the above procedure, for each time interval  $I^i$ ,  $i = 1, \dots, 21$  time-dependent GEV models  $G_{\hat{p}^i, \hat{q}^i}(\mathbf{z}^i)$  with parameters  $(\hat{\mu}^i(t), \hat{\sigma}^i(t), \hat{\xi}^i)$  are inferred from the data block  $\mathbf{z}^i$ . Model  $G_{\hat{p}^i, \hat{q}^i}(\mathbf{z}^i)$  (denoted for shortness  $G_{\hat{p}^i, \hat{q}^i}$  in the rest of this section) is the best estimate for the  $i$ -th data block, relative to the family of models  $G_{p,q}$ . Choosing a model with different orders  $(p, q)$  would either give poor results in the graphical checks, or fail to pass the likelihood ratio test. An example is given in Fig. 1, for the data block  $i = 8$  in the time series with  $\Delta T_E = 2/(1000 \text{ years})$ . The best estimate model has orders  $(\hat{p}^i, \hat{q}^i) = (1, 0)$ . Models  $G_{0,0}$  and  $G_{2,1}$  are rejected, since they have too small likelihood and since the fit quality is very low, as it is illustrated by the probability and quantile plots. On the basis of the diagnostic plots, models  $G_{1,0}$  and  $G_{1,1}$  are both acceptable. However, the deviance statistic satisfies  $\mathcal{D} = 2\{l_{1,1} - l_{1,0}\} = 3.64 < c_{0.5} = 3.84$  which is the 0.95-quantile of the  $\chi_1^2$ -distribution. Therefore, as there is no strong support for selecting model  $G_{1,1}$ , according to the likelihood ratio test the more parsimonious model  $G_{1,0}$  is preferred.

Plots of the best estimate parameters  $(\hat{\mu}^i(t), \hat{\sigma}^i(t), \hat{\xi}^i)$  as functions of time are proposed in Fig. 2. Confidence intervals are computed as the *worst case* estimates: suppose that a model is chosen with  $p = 1$ , that is, for the best estimate  $\mu(t)$  is linear  $\hat{\mu}^i(t) = \mu_0^i + \mu_1^i t$ . Let  $\sigma_{\mu_0^i}$  and  $\sigma_{\mu_1^i}$  be the uncertainties in  $\mu_0^i$  and  $\mu_1^i$ , respectively, provided by the observed information matrix (see Sec. 3). Then the confidence interval at

time  $t$  is computed as

$$[\widehat{\mu}^i(t) - 2(\sigma_{\mu_0^i} + \sigma_{\mu_1^i}t), \widehat{\mu}^i(t) + 2(\sigma_{\mu_0^i} + \sigma_{\mu_1^i}t)]. \quad (20)$$

For most of the time intervals  $I^i$ , the best estimate model is such that  $\widehat{\mu}^i(t)$  and  $\widehat{\sigma}^i(t)$  are respectively linear and constant in time, that is,  $(\widehat{p}^i, \widehat{q}^i) = (1, 0)$ . This is so for all models inferred with the fastest trend intensity  $\Delta T_E = 2/(100 \text{ years})$  (see Tab. 4), whereas for  $\Delta T_E = 2/(300 \text{ years})$  there are two exceptions: intervals  $i = 3$  and  $i = 8$ , for which also  $\widehat{\sigma}^i(t)$  grows linearly in time ( $\widehat{q}^i = 1$ , see Tab. 3). For the slowest trend intensity we obtain  $\widehat{q}^i = 1$  for  $i = 2, 4, 5, 6, 7$  and zero otherwise, whereas  $\widehat{p}^i = 2$  for  $i = 1, 2, 7$  and  $\widehat{p}^i = 1$  otherwise, see Tab. 4. Summarizing, the best fits are mostly achieved by lowest order non-stationary models of the form  $(\widehat{p}^i, \widehat{q}^i) = (1, 0)$ . For slower trends, however, in some cases the best fit is of the form  $(\widehat{p}^i, \widehat{q}^i) = (1, 1)$  or even  $(\widehat{p}^i, \widehat{q}^i) = (2, 1)$ . These cases typically occur for low  $i$ , that is, in the first portion of the time series. This is due to the fact that, for small  $T_E$  (corresponding to small  $t$  through equation (17)), although the hypothesis of smoothness, described in Sec. 2, may still be considered valid, the rate of variation of the SRB measure with respect to variations in  $T_E$  is comparatively larger. To put it in simple words, the statistical behaviour (the attractor) of the baroclinic model is rather sensitive with respect to changes in  $T_E$ . Therefore, the variation of the statistical properties in time is not quite “adiabatic”, in the sense specified in Sec. 2. Correspondingly, a statistical model of enhanced complexity (more parameters) is needed to achieve goodness-of-fit.

In concluding this section, we emphasize that the convergence of the numerical procedure used in the maximization of the likelihood function is here considerably more problematic than in the stationary case studied in Part I. Indeed, in the present case it is often necessary to choose a good starting point for the maximization procedure in order to achieve convergence. For example, in several cases, after achieving convergence for a GEV model with order, say  $(p, q) = (2, 1)$ , by using the inferred values of the parameter vector  $\beta$  in (9) as starting values for the maximization, a better fit (larger likelihood) of *lower order* is obtained. In fact, this has allowed us to reduce the total number of inferences with  $p = 2$  and/or  $q = 1$ .

## 6. Trend assessment

When dealing with non-stationary data, the problem of assessing the sensitivity of trend inferences is particularly delicate. Beyond the serious conceptual problems explained in Sec. 2, one is confronted with several practical issues. Most of the sensitivity tests in Part I were based on examining a shorter portion of same time series or on calculating the maxima on data blocks of different lengths. In the present non-stationary context, both operations would result in an alteration of the statistical properties of the sample (exactly because of the non-stationarity) and this makes comparisons somewhat ambiguous. An example is provided in Fig. 3, where we compute the best estimate GEV fits using sequences of yearly maxima having different lengths – but starting at the same



instant (year 14500) – extracted from the time series with the slowest trend intensity  $\Delta T_E = 2/(1000 \text{ years})$ . Notice that the best fit obtained by taking 100 yearly maxima is stationary. The corresponding extrapolations in time are, of course, completely wrong. By using 500 and 1000 maxima, the best estimates obtained (not shown) fall inside the confidence band of the 2000 years-based estimate for most values of time.

The above example illustrates the *trend dilemma*: on the one hand, in order to be detected, a statistical trend has to be sufficiently fast with respect to the length of the record of observations; on the other hand, if the trend is too fast then the “adiabatic hypothesis” discussed in Sec. 2 is no longer valid: one is left with no “reference statistics” against which the inferred models can be compared.

Moreover, when considering large time spans a further practical complication arises: due to the nonlinear dependence of the statistical properties with respect to the external parameter  $T_E$ , a functional relation between the GEV parameters and time might require many parameters to achieve goodness-of-fit. Therefore, one faces the problem of large uncertainties in the parameter estimates or even lack of convergence. This has indeed been observed for the present time series: if we consider a long record, such that the change in  $T_E$  is large, the model family  $G_{p,q}$  with parameters as in (8) becomes inadequate to catch the time dependence of the statistics of extremes. A first indication of this was reported at the end of Sec. 5. As a further example, we have examined a data block of length 5000 starting at year 14500 in the time series with  $\Delta T_E = 2/(1000 \text{ years})$ . Inspection of graphical diagnostics (probability and quantile plots) reveals that no model in

the family  $G_{p,q}$  produces an acceptable inference. It should be emphasized that goodness-of-fit is achieved for the *same* time series using blocks of length 1000, that is, performing inferences that are more localized in time. So in this case the problem is not the failure of the “adiabatic” or smoothness hypothesis, but the nonlinear dependence of the attractor on the parameter  $T_E$ , which manifests itself on sufficiently large time intervals.

## 7. Smooth dependence on the forcing

The set-up of the present analysis (see Sec. 4) has been chosen to allow comparison of the non-stationary GEV inferences with the results of Part I, obtained from statistically stationary time series. To perform the comparison, for each  $i = 1, \dots, 21$  the best estimate parameters  $(\widehat{\mu}^i(t), \widehat{\sigma}^i(t), \widehat{\xi}^i)$  inferred from data block  $B^i$  are first expressed as functions of  $T_E$  inside the interval (18). This is achieved by inverting the trend formula (17), (writing time as a function of  $T_E$ ):

$$t(T_E) = \frac{T_E - T_E^0 + 1}{\Delta T_E}, \quad T_E \in [9, 51]. \quad (21)$$

and inserting this into the expression of  $(\widehat{\mu}^i(t), \widehat{\sigma}^i(t), \widehat{\xi}^i)$ . This yields functions that are denoted as  $(\widehat{\mu}^i(T_E), \widehat{\sigma}^i(T_E), \widehat{\xi}^i)$ . These are evaluated at the central point  $T_E^i$  of the interval of definition and plotted in Fig. 4. Confidence intervals are given by the same worst case estimate (20) used for Fig. 2. A rather smooth dependence on  $T_E$  is observed, especially for the GEV parameters  $\mu$  and  $\sigma$ . The location parameter  $\mu$  turns out to be

not very sensitive to changes in the trend intensity, being much more sensibly dependent on variations in  $T_E$ . Moreover its confidence intervals are always very small (relatively to the size of  $\mu$ ).

Denote by  $G_{0,0}(\mathbf{w}^i)$  the time-independent GEV models inferred in Part I from stationary sequences  $\mathbf{w}^i$  of 1000 yearly maxima, computed with  $T_E$  fixed at  $T_E^i$ . Denote as  $\tilde{\mu}^i$ ,  $\tilde{\sigma}^i$ , and  $\tilde{\xi}^i$  the inferred values of the GEV parameters of  $G_{0,0}(\mathbf{w}^i)$ . Since the graphs of the parameters  $\tilde{\mu}^i$ ,  $\tilde{\sigma}^i$ , and  $\tilde{\xi}^i$  versus  $T_E^i$  very closely match those in Fig. 4, comparison with the stationary data is presented under the form of relative differences (Fig. 5). To be precise, on the left column the absolute values of the ratios

$$\frac{\widehat{\mu}^i(T_E^i) - \tilde{\mu}^i}{\widehat{\mu}^i(T_E^i) + \tilde{\mu}^i} \quad (22)$$

are plotted against  $T_E^i$  (similarly for the GEV parameters  $\sigma$  and  $\xi$ ). Remarkable agreement is obtained for the parameter  $\mu$ : the relative differences less than 10% and drop below 5% for large  $T_E$  and for all considered trend intensities. Excellent agreement is also obtained for  $\sigma$  (particularly for large  $T_E$ ) and for  $\xi$  except for the fastest trend intensity  $\Delta T_E = 2/(100 \text{ years})$ . In the latter case, indeed, the sample uncertainty is as large as (or even larger than) the estimates self.

We emphasize that inferring time-independent models  $G_{0,0}(\mathbf{z}^i)$  from the non-stationary data  $\mathbf{z}^i$  would induce very large errors (particularly in the scale and shape parameters), compare Fig. 1. A much better (even surprising) agreement between the stationary and

non-stationary estimates is obtained with the procedure described in the previous section: first fitting the time-dependent model  $G_{\hat{p}^i, \hat{q}^i}(z^i)$  and then evaluating its parameters at the central point  $T_E^i$ . There is agreement even in the estimates of the parameter  $\xi$ , which is usually the most difficult one to infer. Indeed, the inferred values are negative. In the case of stationary time series, since the attractor is bounded and since the energy observable  $E(t)$  is a continuous function of the phase space variables, the total energy is bounded on any orbit lying on (or converging to) the attractor. Therefore, the total energy extremes are *necessarily* Weibull distributed ( $\xi$  is negative) Part I. Although this property is not bound to hold for non-stationary forcing, it is still verified, see Tab. 2.

Two distinct power law regimes are identified for the GEV parameters  $(\hat{\mu}^i, \hat{\sigma}^i, \hat{\xi}^i)$  as functions of  $T_E^i$ , having the form

$$\hat{\mu}^i(T_E^i) = \alpha_\mu (T_E^i)^{\gamma_\mu} \quad \text{and} \quad \hat{\sigma}^i(T_E^i) = \alpha_\sigma (T_E^i)^{\gamma_\sigma}, \quad (23)$$

see Fig. 6 and Fig. 7. The values of the fitted exponents  $\gamma_\mu$  and  $\gamma_\sigma$  in each scaling regime are reported in Tab. 5 and Tab. 6, respectively. A similar power law dependence of the GEV parameters on  $T_E$  was already observed in Part I for the stationary data sets  $w^i$ : indeed, the exponents obtained there are very similar to those in Tab. 5 and Tab. 6, particularly for large  $T_E$ . The lack of a power-law scaling regime for the parameter  $\sigma$  for small  $T_E$  explains both the more pronounced differences between the stationary and non-stationary estimates (Fig. 5) and the necessity of including a quadratic term in  $\mu$  and/or a

linear term for  $\sigma$  in the statistical model to get acceptable inferences. This highlights the strongly nonlinear behaviour of the baroclinic model, whose response to changes of  $T_E$  has different features depending on the considered range of variation.

Two factors explain the qualitative analogies and the quantitative agreements between the time-dependent models discussed here and the stationary results of Part I. First of all, the trend intensity imposed on  $T_E$  in all cases is sufficiently slow with respect to the time of relaxation of the baroclinic model to the statistics of extreme values of the total energy. For clarity, we emphasize that the latter time scale is that used in Sec. 2 to define the “adiabatic” hypothesis: it is the time necessary to obtain a good sampling of the SRB measure on the attractor, provided that one may consider the system as “frozen” (with constant  $T_E$ ) for sufficiently long time spans. We do not know whether this time scale bears any physical relation with other time scales, such as those of baroclinic instability or low-frequency variability (both have been described in Speranza and Malguzzi (1988) for the present model). The second factor is that the system’s statistical behaviour responds rather smoothly to the imposed time-dependent variation of the parameter  $T_E$ . This smooth dependence on  $T_E$  of the statistical properties of the baroclinic model was analyzed in detail in Lucarini et al. (2006c,d) by considering not only global physical quantities such as total energy and average wind profiles, but also finer dynamical indicators, such as the Lyapunov exponents and dimension. Both properties of smoothness and “adiabaticity” are of crucial importance in order to justify the usage of non-stationary GEV models that are (locally) smooth functions of time, such as our polynomial family

$G_{p,q}$ .

## 8. Summary and Conclusions

In this paper we have proposed a general, although not universal, framework for the analysis of trends in extremes of climatic time series. When all the shortcomings which are present in datasets and observations have to be considered, a rigorous definition of extremes and a neat, clean, and legible approach to the evaluation of trends is necessary in order to get useful and reliable information (Zhang et al. 2005). The time-dependent approach allows to express the inferred GEV distributional parameters as functions of time. As expected, it is found that trend in the statistics of extreme values is detectable in a reliable way, provided that the record of observations is sufficiently long, depending on the time scale of the trend itself. Trend inference and assessment is much more problematic than in the statistically stationary inference. First of all, one is faced with a serious conceptual problem: there is no “operational” definition of probability, since, to say it in loose words, the time series is not a sampling of a unique probability distribution, as it is in the stationary case. Even if one assumes that the time series is a realization of a sequence of random variables (with different distributions), the statistical properties of the sample are altered by any operation such as resampling or taking shorter subsamples, which makes sensitivity studies somewhat ambiguous. One must assume that the distributions of the random variables vary slowly and smoothly with time, so that

the time series contains sufficient sampling information on the “local” (in time) statistical behaviour.

In the present context, we have adopted GEV models whose parameters are polynomial in time: the location parameter  $\mu$  is at most quadratic with respect to time and the scale parameter  $\sigma$  is at most linear in time. Since the relation between the macroscopic forcing  $T_E$  and time is invertible, the time dependence of the inferred GEV models can be expressed as a relation between the GEV parameters and  $T_E$ , showing rather interesting properties. The location and scale parameters feature power-law dependence with respect to  $T_E$ , while the shape parameter has in all cases a negative value. As expected, both results are in agreement with what obtained in the companion paper (Part I) for stationary data. Since the parameter  $T_E$  increases monotonically in the simulations with the baroclinic model, the system certainly does not possess any invariant measure. However, the results suggest that, as  $T_E$  increases, the system explores statistical states which vary smoothly with  $T_E$  and whose properties are locally quite similar to those obtained in the stationary setting. This is even captured for the relatively fast trend intensity  $\Delta T_E = 2/(100 \text{ years})$ . The proposed explanation is that:

1. the system’s statistical properties depend rather smoothly on  $T_E$  (also compare (Lucarini et al. 2006c,d));
2. the adopted time-scales of variation of  $T_E$  (*i.e.*, the trend intensity  $\Delta T_E$ ) are sufficiently slow compared to the relaxation time to the statistics of extreme values.

The second condition, that was explained in more detail in Sec. 2, amounts to the heuristic statement that for sufficiently short time spans the system’s statistical properties can be considered *frozen* to those holding for a corresponding value of  $T_E$ . The possibility of using GEV models that are locally smooth (polynomial functions of time) depends essentially on these two conditions. For example, for a system having several bifurcations as the control parameter is changed the time-dependent GEV modeling would be much more complicated. This problem is currently under investigation. However, even if the above two conditions do hold, the inference of time-dependent GEV models is valid locally in time, that is, if the sequences of maxima used for the inference span not too large time periods. For large time spans, indeed, the non-linear response of the baroclinic model to variations in  $T_E$  becomes dominant and polynomial GEV models are no longer suitable. On the other hand, if the sequences of maxima used for the inference are too short (depending on the trend intensity), wrong trend estimates may be obtained.

We conclude by observing that the present and the companion paper (Part I) are devoted not merely to the statistical inference of extremes and their trends but also to explore the possibility of using extreme statistics in diagnosing the dynamical state of a geophysical fluid. Our analysis of the problem reveals, in fact, that diagnostics which is based on “universal” (GEV theorem), robust (smoothness properties), simple (power-law scaling), controllable (low-dimensional parametric) statistical models can help very much in setting up well targeted models of the general circulation, see (Lucarini et al. 2006c,d).

There are several ways in which we plan to extend the present study. First of all, we



have considered a rather global indicator, the total energy of the system. Other choices might be to analyze the wave kinetic energy, the available energy or also the maximum vorticity on the domain of the model, which might behave differently as  $T_E$  is changed. Moreover, there are delicate issues connected with reducing the scale from a global indicator to a local one, such as the value of the wind on a grid point. This brings into play all complications due to the multifractality and the spatial dependence of the process. A further development of the present work is the usage of extreme statistics as a dynamical indicator, in the sense of *process oriented metrics* Lucarini et al. (2006a). All these issues are currently under investigation.

## **Acknowledgments**

The authors are indebted to Nazario Tartaglione for useful conversations. This work has been supported by MIUR PRIN Grant “Gli estremi meteo-climatici nell’area mediterranea: proprietà statistiche e dinamiche”, Italy, 2003.

## References

- Brunetti, M., M. Maugeri, T. Nanni, and A. Navarra, 2002: Droughts and extreme events in regional daily italian precipitation series. *Int. J. Clim.*, **22**, 543–558.
- Brunetti, M., L. Buffoni, F. Mangianti, M. Maugeri, and T. Nanni, 2004: Temperature, precipitation and extreme events during the last century in Italy. *Global and Planetary Change*, **40**, 141–149.
- Castillo, E., 1988: *Extreme Value Theory in Engineering*. Academic Press, 389 pp.
- Coles, S., 2001: *An Introduction to Statistical Modelling of Extremes Values*. Springer-Verlag, 208 pp.
- Diaz, H, and T. Nanni, 2006: Historical reconstruction, climate variability and change in Mediterranean regions. *Il Nuovo Cimento*, **29 C**, 1–2.
- Eckmann, J.-P., and D. Ruelle, 1985: Ergodic theory of chaos and strange attractors. *Rev. Mod. Phys.*, **57**, 617–655.
- Embrechts, P., C. Klüppelberg, and T. Mikosch, 1997: *Modelling Extremal Events for Insurance and Finance*. Springer-Verlag, 645 pp.
- Falk, M., J. Hüsler, and R. Reiss, 1994: *Laws of Small numbers: extremes and rare events*. Birkhauser, 389 pp.

- Felici, M., V. Lucarini, A. Speranza, and R. Vitolo, 2006: Extreme Value Statistics of the Total Energy in an Intermediate Complexity Model of the Mid-latitude Atmospheric Jet. Part I: Stationary case. To appear in *J. Atmos. Sci.* (2006).
- Fisher, R. A., and L. H. C. Tippett, 1928: Limiting Forms of the Frequency Distribution of the Largest or Smallest Number of a Sample. *Proc. Cambridge Phil. Soc.*, **24**, 180–190.
- Galambos, J., 1978: *The Asymptotic Theory of Extreme Order Statistics*. Wiley, 352 pp.
- Gnedenko, B. V., 1943: Sur la distribution limite du terme maximum d'une série aléatoire. *Ann. of Math.*, **44**, 423–453.
- Gumbel, E. J., 1958: *Statistics of Extremes*. Columbia University Press.
- Hüsler, J., 1986: Extreme values of nonstationary random sequences. *J. Appl. Probab.*, **23**, 937–950.
- Jenkinson, A. F., 1955: The frequency distribution of the annual maximum (or minimum) values of meteorological elements. *Quart. J. Roy. Meteor. Soc.*, **81**, 158–171.
- Karl, T. R., R. W. Knight, D. R. Easterling, and R. G. Quayle, 1996: Indices of climate change for the United States. *Bull. Amer. Meteor. Soc.*, **77**, 279–292.
- Karl, T. R., and R. W. Knight, 1998: Secular trend of precipitation amount, frequency, and intensity in the United States. *Bull. Amer. Meteor. Soc.*, **79**, 231–242.

- Katz, R. W., and B. G. Brown, 1992: Extreme events in a changing climate: Variability is more important than averages. *Clim. Chang.*, **21**, 289–302.
- Leadbetter, M. R., 1974: On extreme values in stationary sequences. *Zeitschrift fur Wahrscheinlichkeitstheorie und Verwandte Gebiete*, **28**, 289–303.
- Leadbetter, M. R., 1983: Extremes and local dependence in stationary sequences. *Zeitschrift fur Wahrscheinlichkeitstheorie und Verwandte Gebiete*, **65**, 291–306.
- Lindgren, G., M. R. Leadbetter, and H. Rootzén, 1983: *Extremes and Related Properties of Random Sequences and Processes*. Springer-Verlag, 336 pp.
- Lucarini, V., S. Calmanti, A. dell’Aquila, P. M. Ruti, and A. Speranza, 2006: Intercomparison of the northern hemisphere winter mid-latitude atmospheric variability of the IPCC models. *Preprint ArXiv*, DOI:physics/0601117.
- Lucarini, V., T. Nanni, A. Speranza, 2004: Statistics of the seasonal cycle of the 1951-2000 surface temperature records in Italy. *Il Nuovo Cimento*, **27 C**, 285–298.
- Lucarini, V., A. Speranza, and T. Nanni, 2006: Statistics of the seasonal cycle of the 1951-2000 surface temperature records in Italy and in the Mediterranean area. *Il Nuovo Cimento*, **29 C**, 21–31.
- Lucarini, V., A. Speranza, and R. Vitolo, 2006: Physical and Mathematical Properties of a Quasi-Geostrophic Model of Intermediate Complexity of the Mid-Latitudes Atmospheric Circulation. *Preprint ArXiv*, DOI:physics/0511208.

- V. Lucarini, A. Speranza, R. Vitolo: Self-Scaling of the Statistical Properties of a Minimal Model of the Atmospheric Circulation, to appear in *20 Years of Nonlinear Dynamics in Geosciences*, Eds. J. Elsner, A. Tsonis, Springer (New York, USA) (2006).
- Malguzzi, P., A. Trevisan, and A. Speranza, 1990: Statistic and Predictability for an intermediate dimensionality model of the baroclinic jet. *Annales Geophysicae*, **8**, 29–36.
- Reiss, R.-D., and Thomas, M., 2001: *Statistical Analysis of Extreme Values: with Applications to Insurance, Finance, Hydrology and Other Fields*. 2nd ed., Birkhauser, 443 pp.
- Speranza, A., and P. Malguzzi, 1988: The statistical properties of a zonal jet in a baroclinic atmosphere: a semilinear approach. Part I: two-layer model atmosphere. *J. Atmos. Sci.*, **48**, 3046–3061.
- Speranza, A., A. Delitala, R. Deidda, S. Corsini, G. Monacelli, B. Bonaccorso, A. Buzzi, A. Cancelliere, M. Fiorentino, G. Rossi, P. Ruti, F. Siccardi, 2006: Estremi nelle scienze ambientali. *L'Acqua*, **3/2006**, 19–30.
- Speranza, A., and N. Tartaglione, 2006: Extreme events in the Mediterranean area: A mixed deterministic–statistical approach *Il Nuovo Cimento*, **29 C**, 81–88.
- Tartaglione, N., A. Speranza, F. Dalan, T. Nanni, M. Brunetti, and M. Maugeri, 2006: The mobility of Atlantic baric depressions leading to intense precipitation over Italy: a

- preliminary statistical analysis. Accepted for publication in *Natural Hazards and Earth System Science* (2006).
- Tiago de Oliveira, J., 1984: *Statistical Extremes and Applications*. Kluwer Academic Publishers, 708 pp.
- Watson, R.T., and the Core Writing Team, Eds., 2001: *Climate Change 2001: Synthesis Report. A Contribution of Working Groups I, II, and III to the Third Assessment Report of the Intergovernmental Panel on Climate Change*. Cambridge University Press, 398 pp. [Available at <http://www.ipcc.ch>].
- Young, L.S., 2002: What Are SRB Measures, and Which Dynamical Systems Have Them? *J. Stat. Phys.*, **108**, 733–754.
- Zhang, X., F. W. Zwiers, and G. Li, 2003: Monte Carlo Experiment on the Detection of Trends in Extreme Values. *J. Climate*, **17**, 1945–1952.
- Zhang, X., G. Hegerl, F. W. Zwiers, and J. Kenyon, 2005: Avoiding Inhomogeneity in Percentile-Based Indices of Temperature Extremes. *J. Climate*, **18**, 1641–1651.

## List of Figures

- 1 Diagnostic plots of GEV inferences with model (7) and parameters as in (8), for block  $B_i$  with  $i = 8$  (corresponding to  $T_E^i = 24$ ) and  $\Delta T_E = 2/(1000 \text{ years})$ . Top row: probability plots. Bottom row: quantile plots. From left to right column: plots for models  $G_{p,q}$  (see (8)), with  $(p, q)$  and the corresponding log-likelihood  $l$  (see (6)) indicated on top. . . . . 41
- 2 GEV parameters as functions of time, for the three considered values of trend intensity  $\Delta T_E$ : from top to bottom,  $\Delta T_E = 2/(1000 \text{ years})$ ,  $2/(300 \text{ years})$ , and  $2/(100 \text{ years})$ , respectively. For each trend intensity the inferred time-dependent parameters  $(\mu(t), \sigma(t), \xi)$  (left, center, right column, respectively) of the best estimate model  $G_{\hat{p}^i, \hat{q}^i}(z^i)$  are plotted. . . . . 42
- 3 Parameter  $\mu(t)$  of the best estimate GEV inferences as a function of time. The time series with slowest trend intensity  $\Delta T_E = 2/(1000 \text{ years})$  has been used, taking yearly maxima over a data block starting at year 14001. For legibility, only the confidence intervals have been plotted. Left: inferences obtained with 100, 500, and 1000 yearly maxima. The best estimate fit based on 100 data is stationary ( $\mu_1 = 0$ ) and it has been extrapolated to 500 years. Right: inferences obtained with 500, 1000, and 2000 yearly maxima. In all cases, the best estimate GEV model has  $p = 1$ , that is,  $\mu(t) = \mu_0 + \mu_1 t$  is a linear function of time. . . . . 43

4	Parameters $(\widehat{\mu}^i(T_E^i), \widehat{\sigma}^i(T_E^i), \widehat{\xi}^i)$ (from left to right, respectively) of the best estimate GEV model $G_{\widehat{p}^i, \widehat{q}^i}(z^i)$ evaluated at the central point $T_E^i$ of each of the 21 intervals (18). From top to bottom the trend intensity $\Delta T_E$ is equal to $2/(1000 \text{ years})$ , $2/(300 \text{ years})$ , and $2/(100 \text{ years})$ , respectively. . . . .	44
5	Same as Fig. 4 for the estimates obtained with the stationary data in Part I, see text for details. The time-dependent estimates of Fig. 4 are plotted with dotted lines. . . . .	45
6	Power law fits of the inferred values of $\widehat{\mu}^i(T_E^i)$ as a function of $T_E^i$ (see (19)). From left to right: trend intensities of $2/(1000 \text{ years})$ , $2/(300 \text{ years})$ , and $2/(100 \text{ years})$ have been used. In each case, there are two intervals of $T_E$ characterized by different scaling law, separated by a point $T_E^b$ , compare Tab. 5. . . . .	46
7	Same as Fig. 6 for the inferred values $\widehat{\sigma}^i(T_E^i)$ . . . . .	47



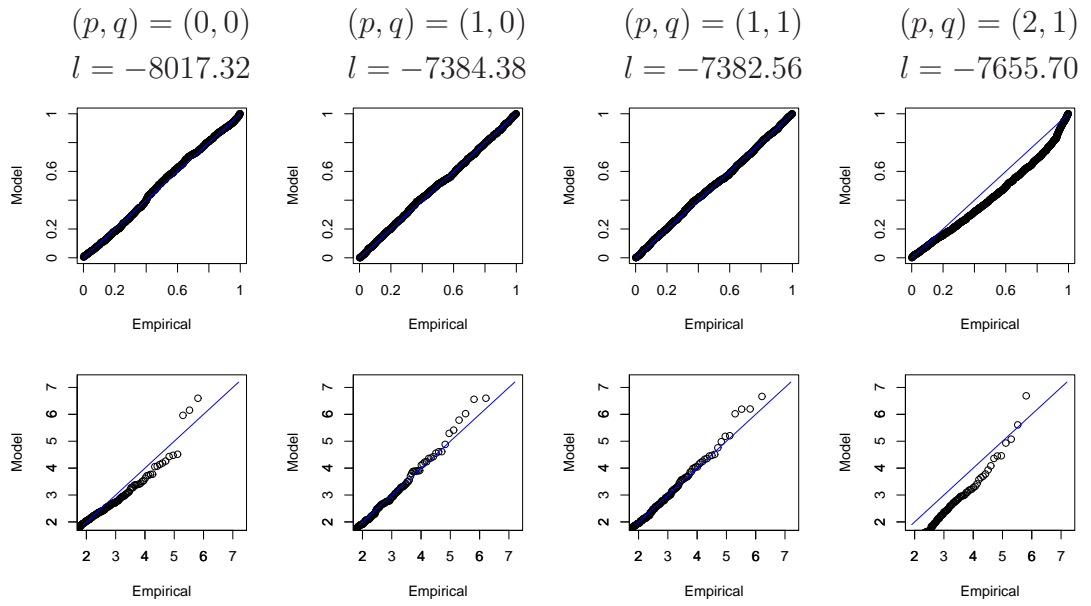


Figure 1: Diagnostic plots of GEV inferences with model (7) and parameters as in (8), for block  $B_i$  with  $i = 8$  (corresponding to  $T_E^i = 24$ ) and  $\Delta T_E = 2/(1000 \text{ years})$ . Top row: probability plots. Bottom row: quantile plots. From left to right column: plots for models  $G_{p,q}$  (see (8)), with  $(p, q)$  and the corresponding log-likelihood  $l$  (see (6)) indicated on top.

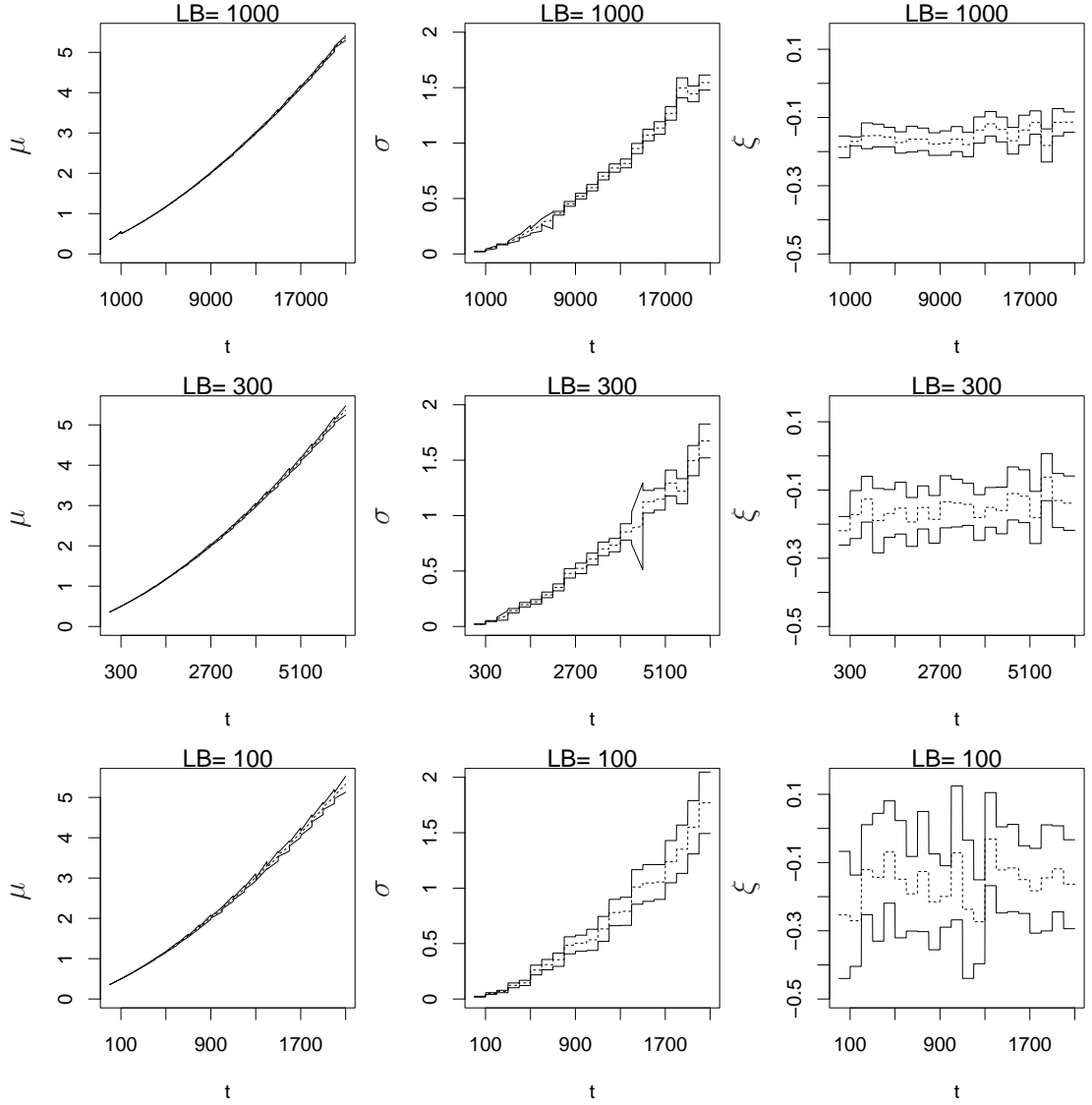


Figure 2: GEV parameters as functions of time, for the three considered values of trend intensity  $\Delta T_E$ : from top to bottom,  $\Delta T_E = 2/(1000 \text{ years})$ ,  $2/(300 \text{ years})$ , and  $2/(100 \text{ years})$ , respectively. For each trend intensity the inferred time-dependent parameters  $(\mu(t), \sigma(t), \xi)$  (left, center, right column, respectively) of the best estimate model  $G_{\hat{p}^i, \hat{q}^i}(z^i)$  are plotted.

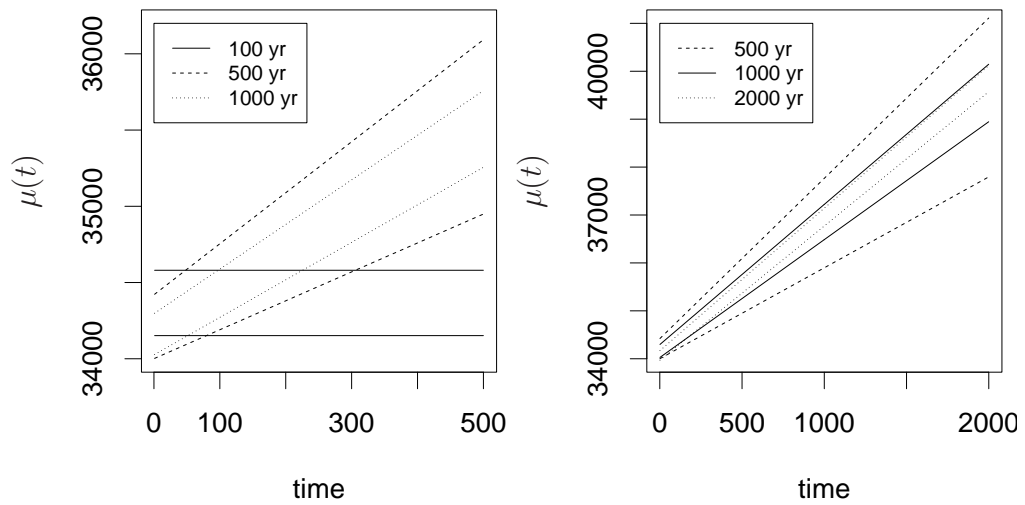


Figure 3: Parameter  $\mu(t)$  of the best estimate GEV inferences as a function of time. The time series with slowest trend intensity  $\Delta T_E = 2/(1000 \text{ years})$  has been used, taking yearly maxima over a data block starting at year 14001. For legibility, only the confidence intervals have been plotted. Left: inferences obtained with 100, 500, and 1000 yearly maxima. The best estimate fit based on 100 data is stationary ( $\mu_1 = 0$ ) and it has been extrapolated to 500 years. Right: inferences obtained with 500, 1000, and 2000 yearly maxima. In all cases, the best estimate GEV model has  $p = 1$ , that is,  $\mu(t) = \mu_0 + \mu_1 t$  is a linear function of time.

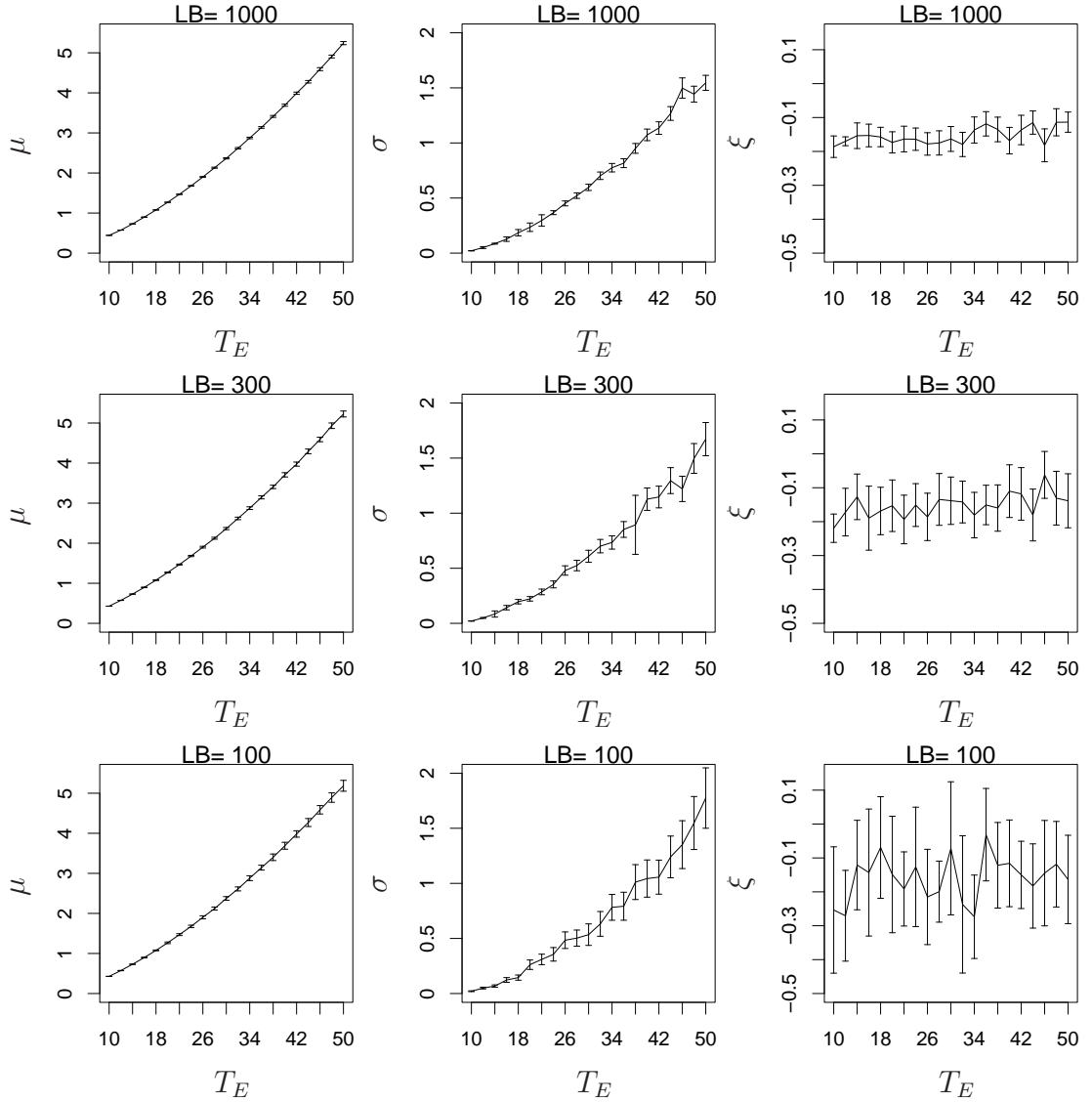


Figure 4: Parameters  $(\hat{\mu}^i(T_E^i), \hat{\sigma}^i(T_E^i), \hat{\xi}^i)$  (from left to right, respectively) of the best estimate GEV model  $G_{\hat{p}^i, \hat{q}^i}(z^i)$  evaluated at the central point  $T_E^i$  of each of the 21 intervals (18). From top to bottom the trend intensity  $\Delta T_E$  is equal to  $2/(1000 \text{ years})$ ,  $2/(300 \text{ years})$ , and  $2/(100 \text{ years})$ , respectively.

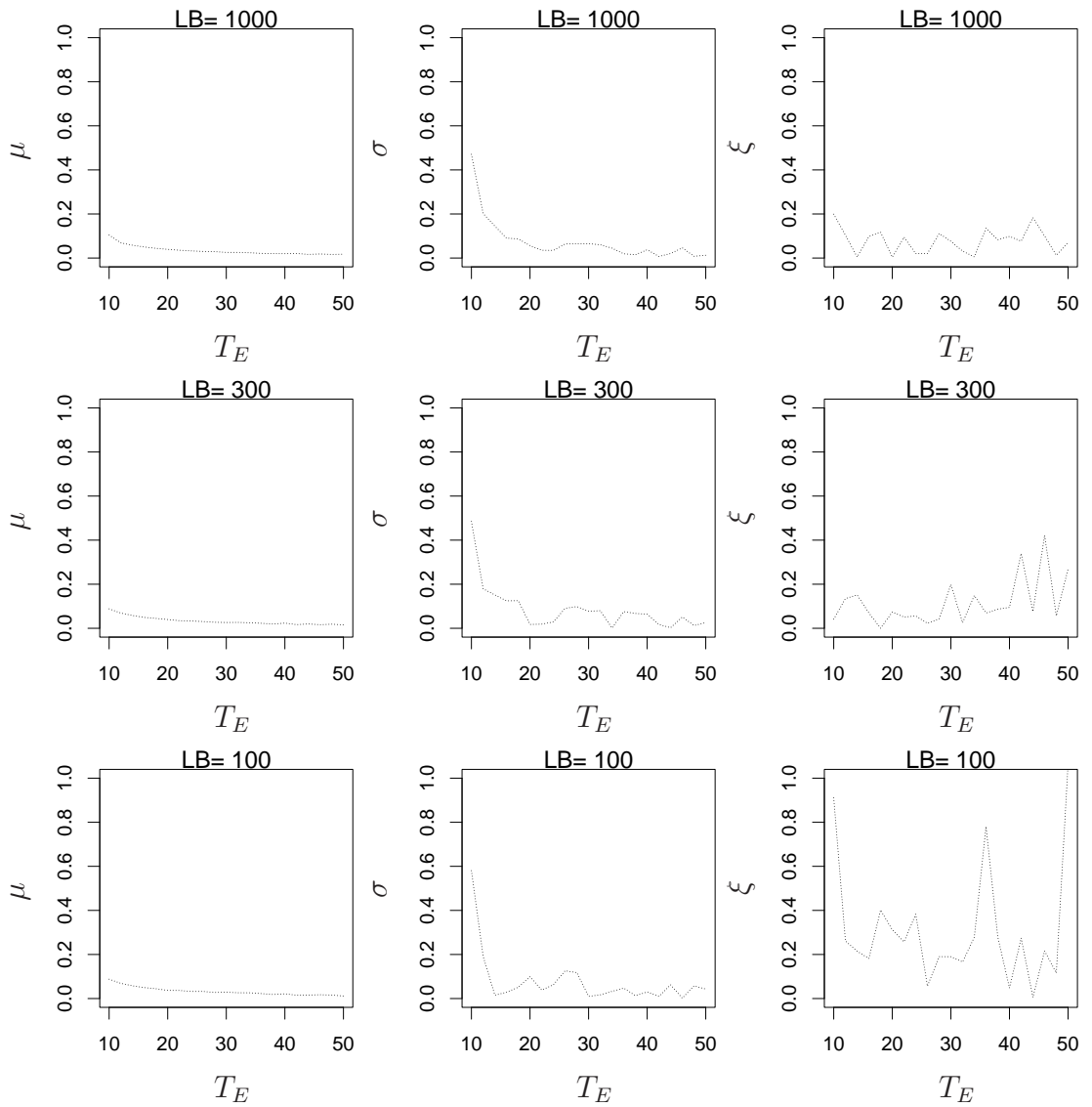


Figure 5: Same as Fig. 4 for the estimates obtained with the stationary data in Part I, see text for details. The time-dependent estimates of Fig. 4 are plotted with dotted lines.

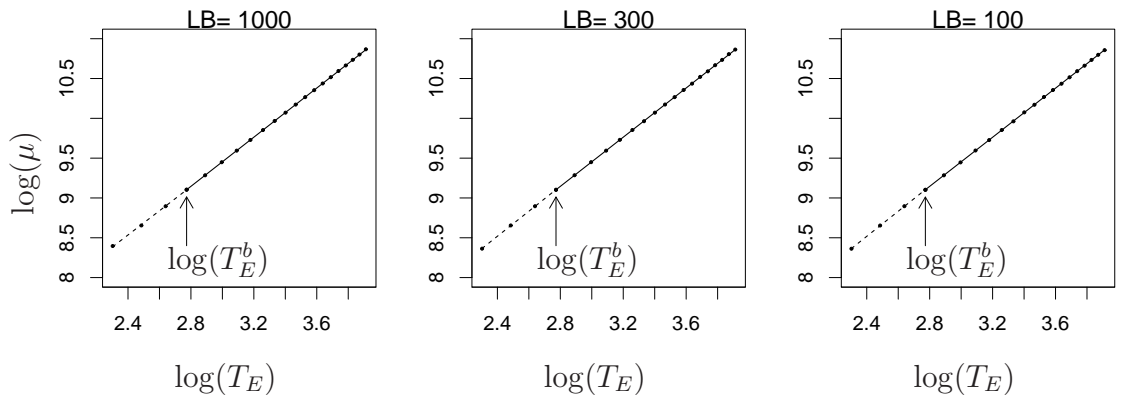


Figure 6: Power law fits of the inferred values of  $\hat{\mu}^i(T_E^i)$  as a function of  $T_E^i$  (see (19)). From left to right: trend intensities of  $2/(1000 \text{ years})$ ,  $2/(300 \text{ years})$ , and  $2/(100 \text{ years})$  have been used. In each case, there are two intervals of  $T_E$  characterized by different scaling law, separated by a point  $T_E^b$ , compare Tab. 5.

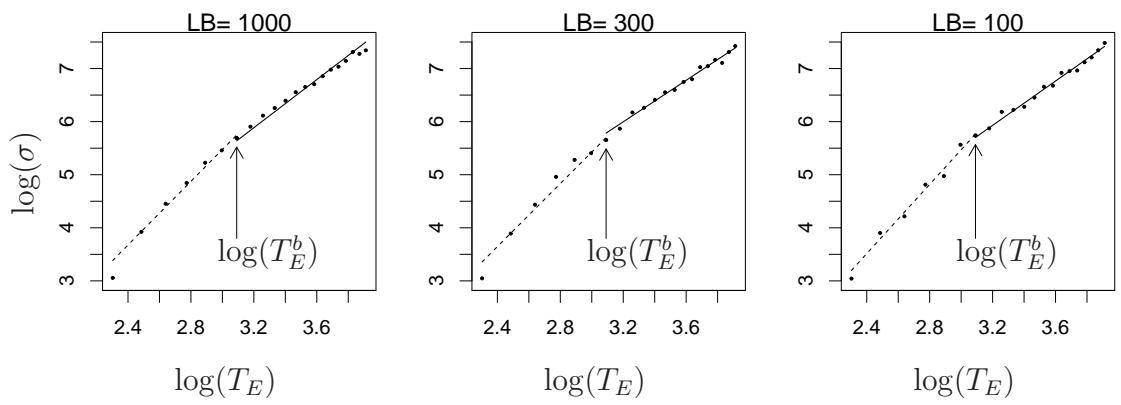


Figure 7: Same as Fig. 6 for the inferred values  $\hat{\sigma}^i(T_E^i)$ .

$\Delta T_E$	2/1000	2/300	2/100
$L$	21000	6300	2100
$L_B$	1000	300	100

Table 1: The length  $L$  of each of the three time series and the length  $L_B$  of each of the 21 the data blocks  $B_i$  (both are expressed in years), as a function of the intensity  $\Delta T_E$  of the trend (17) imposed on the parameter  $T_E$  of the baroclinic model.



$i$	$\hat{\mu}_0$	$\hat{\mu}_1$	$\hat{\mu}_2$	$\hat{\sigma}_0$	$\hat{\sigma}_1$	$\hat{\xi}$
1	3585.5	1.40	5.8e-04	21.3	0	-0.19
2	5018.9	1.39	9.0e-05	39.3	0.022	-0.17
3	6497.8	1.61	0	85.9	0	-0.15
4	8106.6	1.77	0	105.6	0.043	-0.15
5	9851.7	1.84	0	155.5	0.060	-0.16
6	11709.6	1.96	0	206.8	0.055	-0.17
7	13733.7	1.79	2.1e-04	290.2	0.011	-0.16
8	15718.9	2.14	0	367.4	0	-0.16
9	17935.6	2.15	0	451.3	0	-0.18
10	20141.2	2.35	0	521.6	0	-0.17
11	22527.4	2.25	0	597.4	0	-0.16
12	24934.5	2.48	0	702.2	0	-0.18
13	27452.0	2.58	0	774.7	0	-0.14
14	30067.3	2.59	0	816.2	0	-0.12
15	32696.9	2.85	0	951.0	0	-0.14
16	35348.0	3.16	0	1072.7	0	-0.17
17	38382.8	3.06	0	1136.1	0	-0.14
18	41348.7	2.85	0	1267.9	0	-0.11
19	44351.3	3.16	0	1498.3	0	-0.18
20	47502.7	3.15	0	1444.3	0	-0.11
21	51288.4	2.26	0	1545.9	0	-0.11

Table 2: Best estimate GEV fits  $G_{\hat{p}^i, \hat{q}^i}(z^i)$  with parameter vector as in (9) for the non-stationary time series with trend intensity  $\Delta T_E = 2/(1000 \text{ years})$ , see text for details.

$i$	$\hat{\mu}_0$	$\hat{\mu}_1$	$\hat{\mu}_2$	$\hat{\sigma}_0$	$\hat{\sigma}_1$	$\hat{\xi}$
1	3583.7	4.69	0	21.1	0	-0.22
2	4988.2	5.00	0	48.9	0	-0.17
3	6490.9	5.41	0	68.8	0.104	-0.13
4	8050.0	6.18	0	142.6	0	-0.19
5	9798.6	6.52	0	196.4	0	-0.17
6	11735.9	6.45	0	222.6	0	-0.15
7	13750.8	6.20	0	285.4	0	-0.19
8	15763.2	6.97	0	353.0	0	-0.15
9	17844.1	7.86	0	479.5	0	-0.19
10	20108.0	7.57	0	524.3	0	-0.13
11	22485.1	7.75	0	607.9	0	-0.14
12	24954.8	8.26	0	700.3	0	-0.14
13	27386.1	9.06	0	733.9	0	-0.18
14	29928.5	10.07	0	852.9	0	-0.15
15	32724.5	8.88	0	888.0	0.054	-0.16
16	35671.6	9.36	0	1125.4	0	-0.11
17	38284.6	9.72	0	1147.4	0	-0.12
18	41436.1	9.96	0	1294.0	0	-0.18
19	44387.2	10.05	0	1220.3	0	-0.06
20	47706.3	10.77	0	1496.0	0	-0.13
21	50890.5	9.09	0	1673.7	0	-0.14

Table 3: As in Tab. 2 for trend intensity  $\Delta T_E = 2/(300 \text{ years})$ .

$i$	$\hat{\mu}_0$	$\hat{\mu}_1$	$\hat{\mu}_2$	$\hat{\sigma}_0$	$\hat{\sigma}_1$	$\hat{\xi}$
1	3572.1	14.22	0	21.0	0	-0.25
2	4986.8	14.91	0	49.6	0	-0.27
3	6485.6	16.40	0	67.7	0	-0.12
4	8118.5	17.11	0	123.1	0	-0.14
5	9905.1	17.29	0	144.9	0	-0.07
6	11679.7	19.66	0	261.3	0	-0.15
7	13628.2	21.49	0	309.9	0	-0.19
8	15542.3	24.39	0	354.5	0	-0.13
9	17757.6	25.41	0	484.3	0	-0.22
10	20246.2	19.26	0	503.4	0	-0.20
11	22556.3	23.61	0	533.9	0	-0.07
12	24848.3	25.25	0	632.3	0	-0.24
13	27441.5	27.18	0	780.3	0	-0.27
14	29638.6	35.68	0	791.0	0	-0.03
15	32617.7	28.06	0	1010.6	0	-0.12
16	35813.0	21.47	0	1046.2	0	-0.12
17	38422.4	28.22	0	1055.2	0	-0.15
18	41119.7	31.07	0	1238.6	0	-0.18
19	44510.3	27.28	0	1351.2	0	-0.14
20	47640.6	25.50	0	1548.8	0	-0.12
21	50454.4	28.14	0	1769.8	0	-0.16

Table 4: As in Tab. 2 for trend intensity  $\Delta T_E = 2/(100 \text{ years})$ .

$L_B$	$\gamma_{\mu,1}$	$T_E^b$	$\gamma_{\mu,2}$
1000	$1.5200 \pm 0.0041$	16	$1.5434 \pm 0.0042$
300	$1.5706 \pm 0.0091$	16	$1.5452 \pm 0.0072$
100	$1.5733 \pm 0.0125$	16	$1.5419 \pm 0.0129$

Table 5: Power law fits of the inferred location parameter  $\widehat{\mu}^i(T_E^i)$  as a function of  $T_E^i$  (see (19)) of the form  $\widehat{\mu}^i(T_E^i) = \alpha_\mu(T_E^i)^{\gamma_\mu}$ . Two distinct scaling regimes (with distinct exponents  $\gamma_{\mu,1}$  and  $\gamma_{\mu,2}$ ) are identified and the corresponding adjacent intervals in the  $T_E$ -axis are separated by  $T_E^b$ .

$L_B$	$\gamma_{\sigma,1}$	$T_E^b$	$\gamma_{\sigma,2}$
1000	$3.5212 \pm 0.1600$	18	$2.1000 \pm 0.0725$
300	$3.9180 \pm 0.3142$	16	$2.1055 \pm 0.0580$
100	$3.2351 \pm 0.2154$	22	$2.0891 \pm 0.1797$

Table 6: Same as Tab. 5 for the inferred scale parameter  $\hat{\sigma}^i(T_E^i)$ .